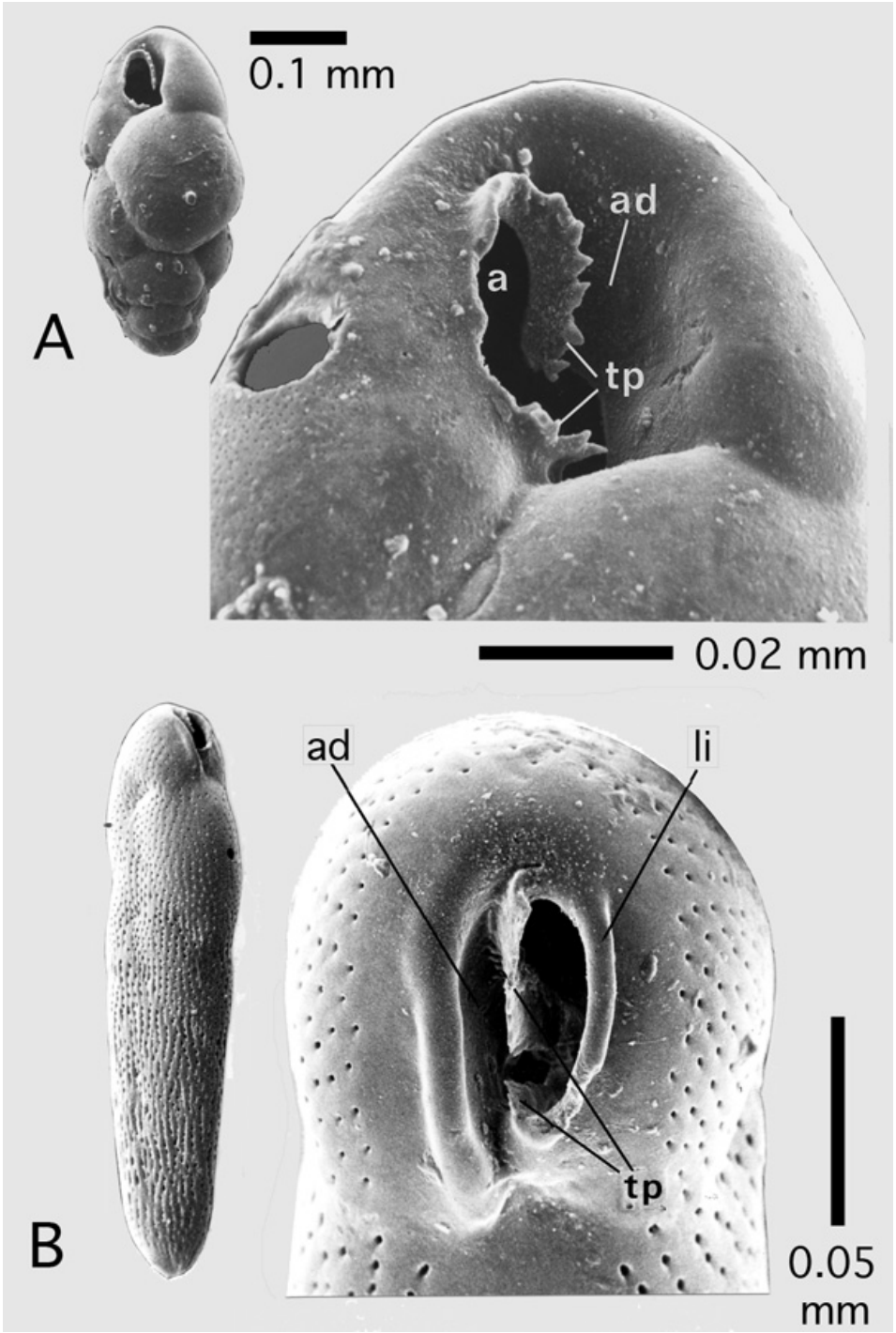

Figure 2: Adapertural depression and toothplate with serrated margin. SEM, from HOTTINGER *et alii*, 1993.
A: *Bulimina elongata* d'ORBIGNY; **B:** *Loxostomina* cf. *africana* (SMITTER).
a: aperture; **ad:** adapertural depression; **li:** lip; **tp:** toothplate with its serrated margin.

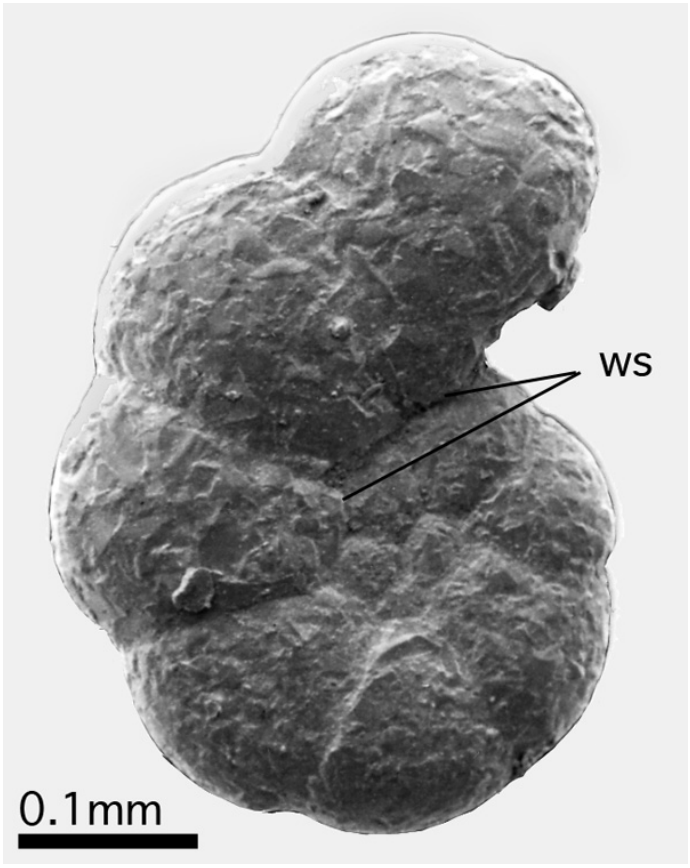

Figure 3: Advolute whorl in agglutinated planispiral shell of *Labrospira jeffreysii* (WILLIAMSON). SEM, from HOTTINGER *et alii*, 1993.
ws: whorl suture.

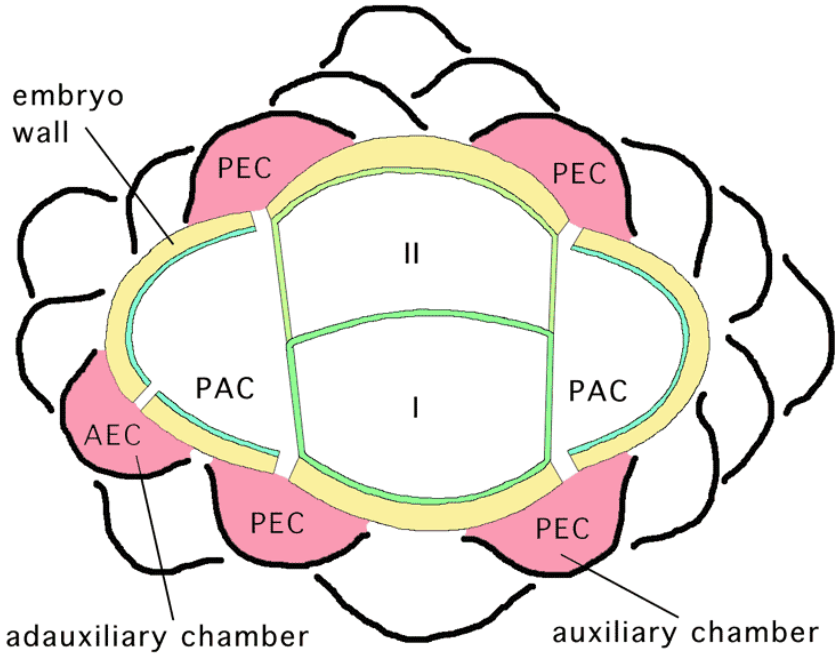

Figure 4: Embryonic and periembryonic chambers in *Orbitoides* spp. according to VAN HINTE's 1966 concept.
I: protoconch; **II:** deuteroconch; **PAC:** principal auxiliary chamber; **PEC:** principal epi-auxiliary chamber; **AEC:** accessory epi-auxiliary chamber. In our view, we prefer to call PAC an auxiliary and AEC an adauxiliary chamber.

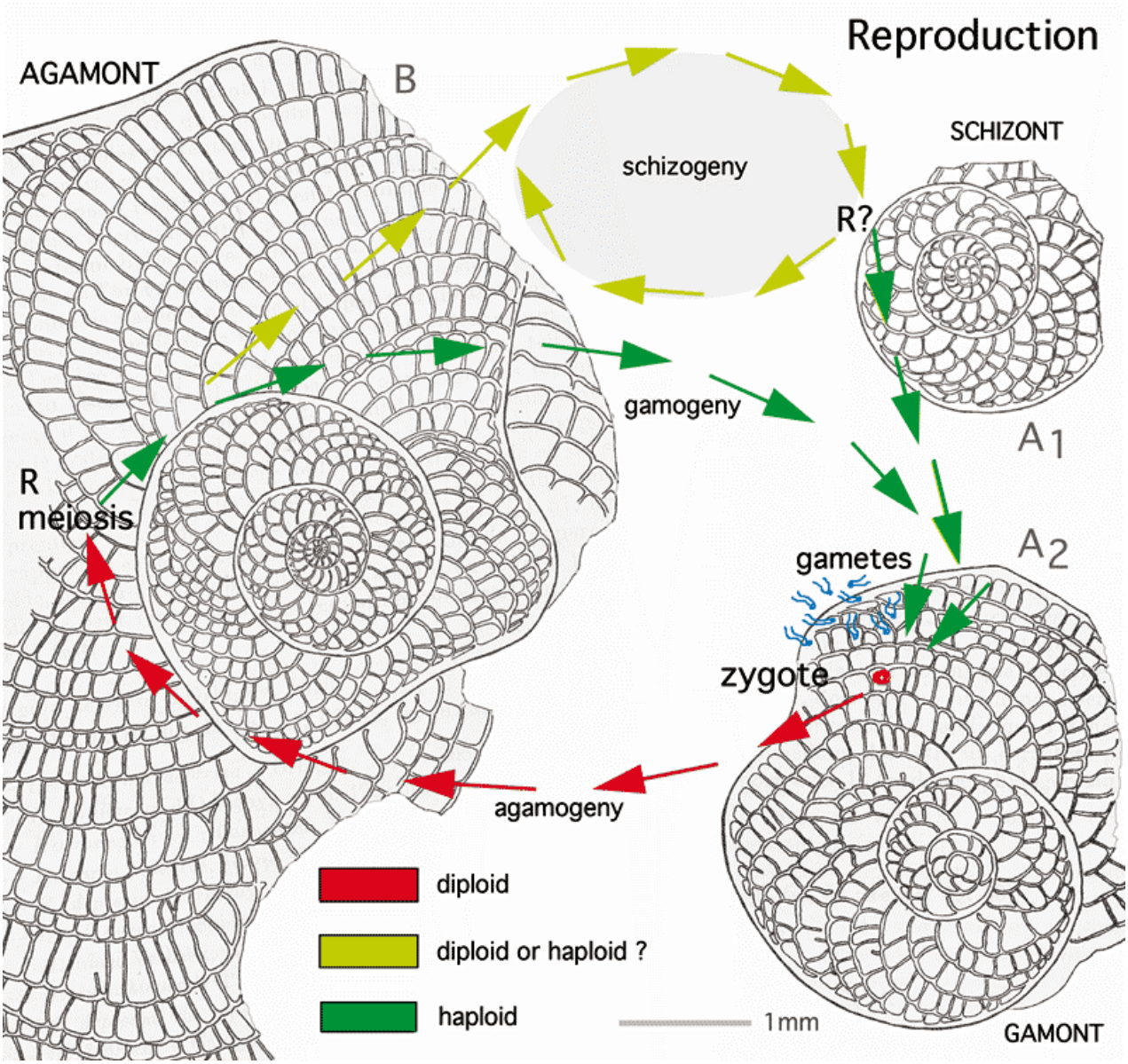

Figure 5: Standard dimorphic or trimorphic reproductive cycle in benthic, medium- to large-sized foraminifera according to GOLDSTEIN, 1999. Schizogeny, eventually repeated several times, may be widespread in larger foraminifera from oligotrophic habitats. Planktic foraminifera seem to have no dimorphic life cycle. Life cycles are linked in various ways to seasonal cycles. Example: *Heterostegina depressa* d'ORBIGNY, equatorial sections, Gulf of Aqaba, Red Sea (from HOTTINGER, 1977).

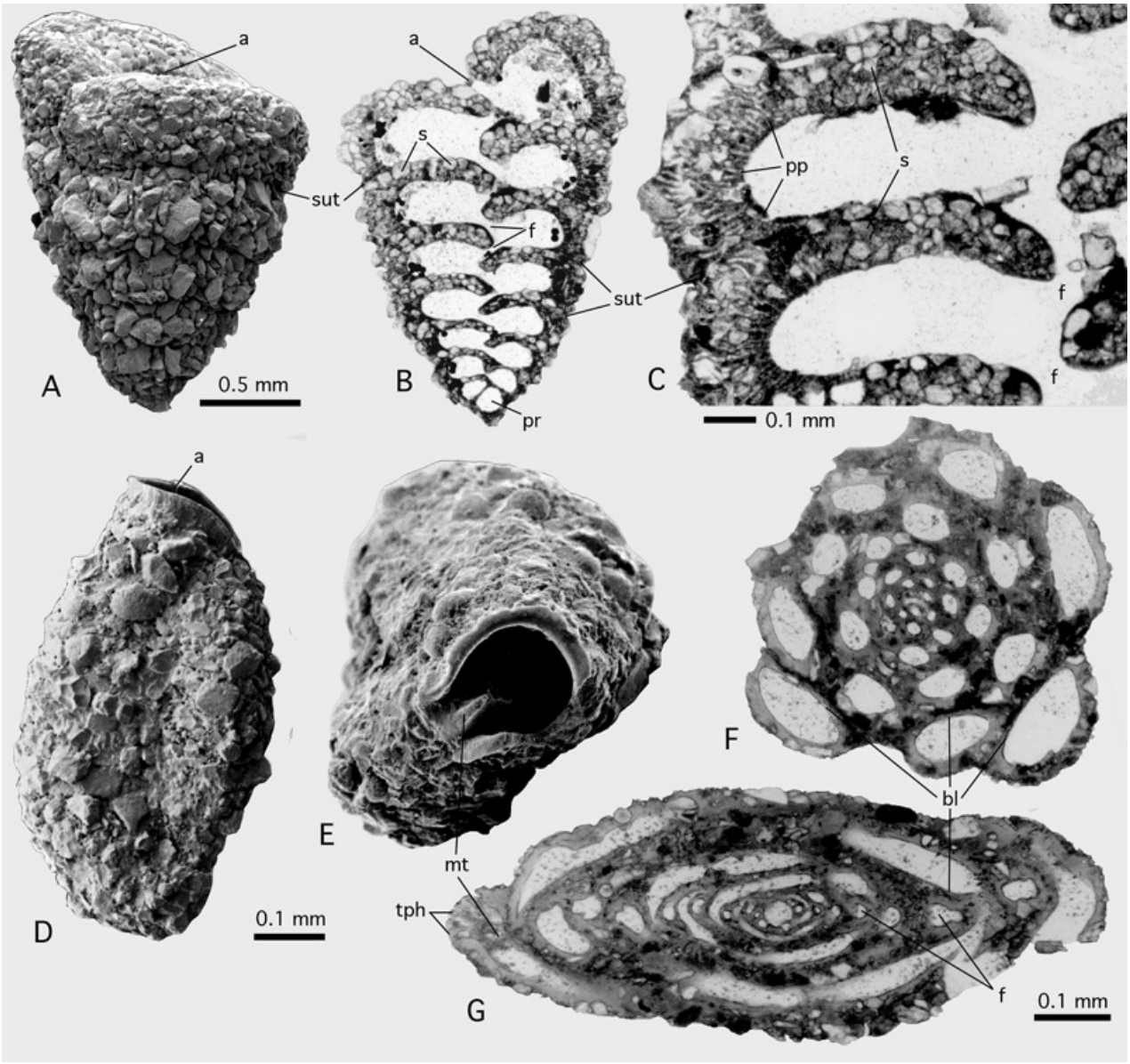

Figure 6: Agglutination in foraminiferan walls; Gulf of Aqaba, Red Sea; Recent.
A-C: *Textularia* sp. C in HOTTINGER *et alii*, 1993. **A:** Lateral view showing coarse grains producing a rugged shell surface exept on apertural face. SEM. **B:** axial thin section of the biserial test showing distribution of agglutinated grains within the shell walls. Light microscope, transparent light. **C:** Detail from another specimen showing parapore texture of wall and its relation to the agglutinated grains. Transmitted light. **D-G:** *Agglutinella* sp., an agglutinating, porcelaneous miliolid. **D:** lateral view showing coarse agglutination at the shell's suface. **E:** apertural view showing large aperture with a porcelaneous peristomal rim and a miliolid tooth. SEM. **F-G:** *Schlumbergerina alveoliniformis* (BRADY), thin sections in the - and perpendicular to the - apertural axis, showing early growth stages without apparent agglutination and a very thin basal layer coating the rugged surface of adult chambers of the previous whorl. Transmitted light.
a: aperture; **bl:** basal layer; **f:** foramen; **mt:** miliolid tooth; **pp:** parapores; **pr:** proloculus; **s:** septum; **sut:** (chamber) suture; **tph:** trematophore.

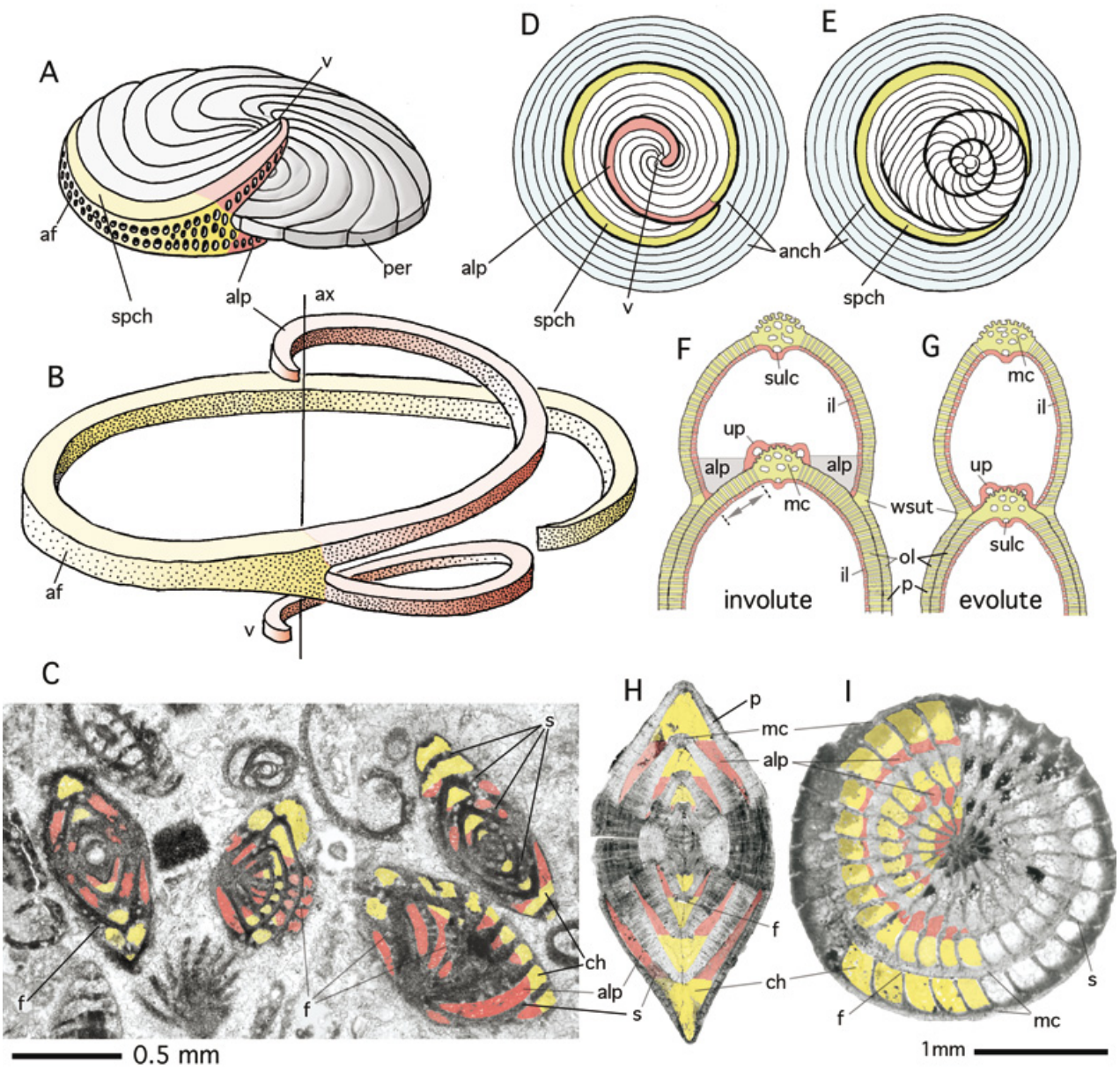

Figure 7: Alar prolongations and involuteness in lamellar foraminifers.
A: planispiral-involute shell with a long apertural face, as in *Archaias*. Note the apertures in the face of both alar prolongations. **B:** shape of single (penultimate) spiral chamber with long alar prolongations forming a vortex. **C:** Random sections of "*Peneroplis*" *glynnjonesi* HENSON, Lower Oligocene, Iran. Transmitted light. Note foramina in the alar septa. **D-E:** Transition from planispiral-involute to annular growth. **D:** external, lateral view of subsequent chambers, showing the ultimate spiral chamber with its alar prolongation and subsequent annular chambers. **E:** all chambers in equatorial section including the tightly coiled nepiont. **F-G:** Involuteness and evoluteness in lamellar foraminifers: an accurate definition is whether or not perforate walls (double arrow) cover the next whorl. Axial section, schematic, not to scale. Note the numerous, outer lamellas (green) enveloping the total exposed surface of the previous shell (compare "lamellation"). The distribution of the inner lamella (red) covering the previous whorl hasno significance in the definition of involuteness. **H-I:** *Nummulites incrassatus* DE LA HARPE. Upper Eocene, Northern Italy. **H:** not quite centered axial section.
Red: lumen of alar prolongation, **yellow:** lumen of equatorial chamber. **I:** oblique section almost perpendicular to shell axis. Note the obliqueness of the intersections of the alar prolongations.
af: apertural face; **alp:** alar prolongation; **anch:** annular chambers; **ax:** shell axis; **ch:** chamber; **f:** foramen; **il:** inner lamella; **mc:** marginal cord; **ol:** (numerous) outer lamellas; **p:** pore; **per:** periphery (of spiral shell); **s:** septum; **spch:** spiral chamber; **sulc:** sulcus; **v:** vortex; **wsut:** whorl suture.

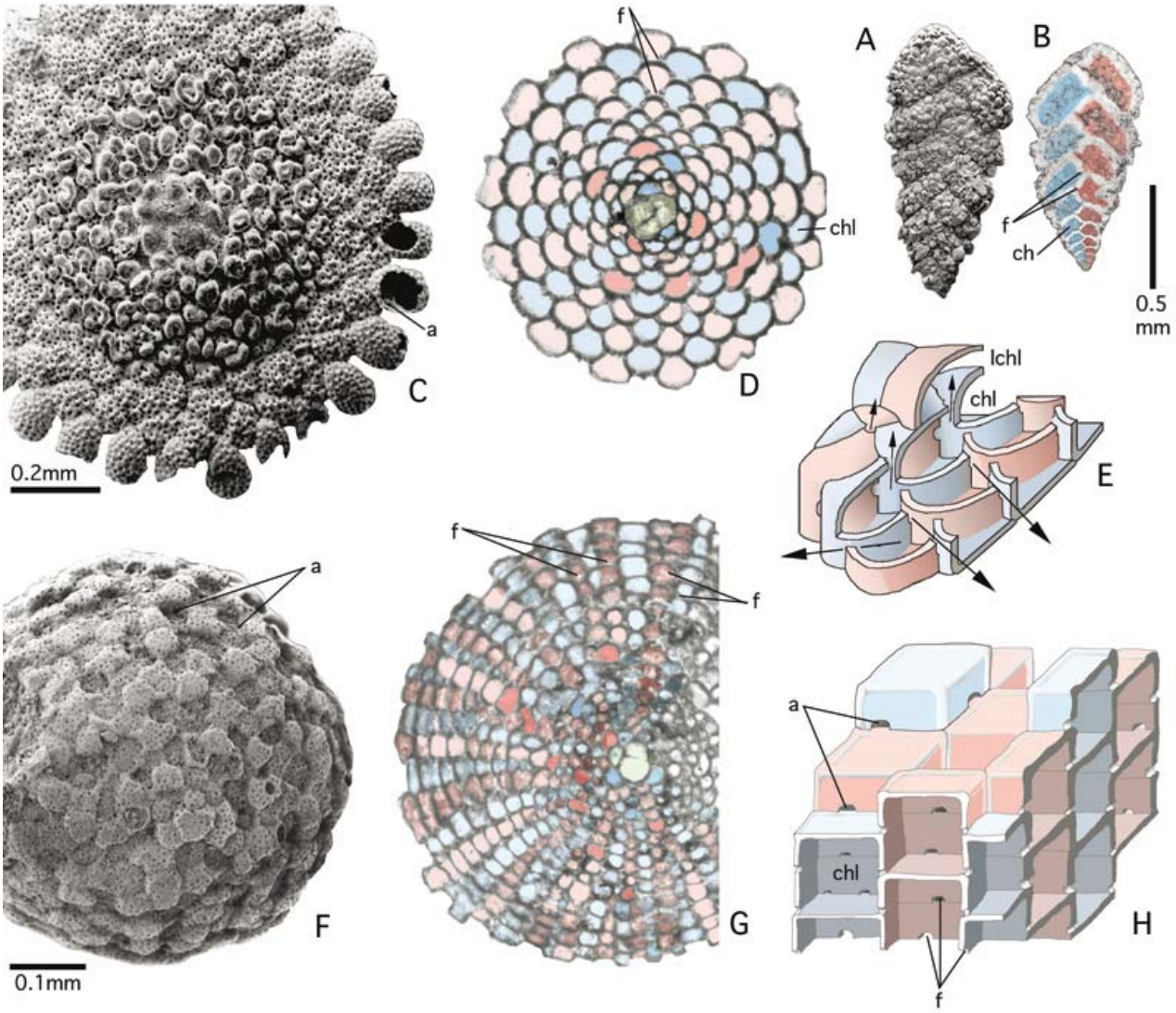

Figure 8: Alternating arrangement of shell compartments in the three dimensions of space. Examples from Gulf of Aqaba, Red Sea; Recent.
A-B: Alternating chamber arrangement in the linear dimension (= **biserial** arrangement) as in *Textularia foliacea* HERON-ALLEN et EARLAND, SEM and X-ray graphs of lateral view. **C-D:** Alternating chamberlet arrangement in the planar (second) dimension, as in annular-concentric, discoidal shell of *Planorbulinella elatensis* THOMAS, SEM graph of lateral view and equatorial section in transmitted light microscopy, coloured. **E:** Stereograph showing alternating chamberlets of a main chamberlet layer, with main stolon axes (horizontal arrows) and retrovert stolons feeding lateral chamberlet (vertical arrows). Schematic, not to scale. **F-G:** Alternating chamberlet arrangement in the third dimension producing a chessboard pattern, as in the spherical-concentric, globular shell of *Sphaerogypsina globulus* (REUSS), SEM graph of external view and centered section in transmitted light micrograph, coloured. **H:** Stereograph showing alternating chamberlets forming **chessboard pattern**. Schematic, not to scale.
Colours: **red** and **blue:** alternating generations of shell compartments; **green:** nepiontic, early stages including proloculus.
a; aperture; **ch:** chamber lumen; **chl:** chamberlet lumen; **f:** foramen; **lchl:** lateral chamberlet lumen.

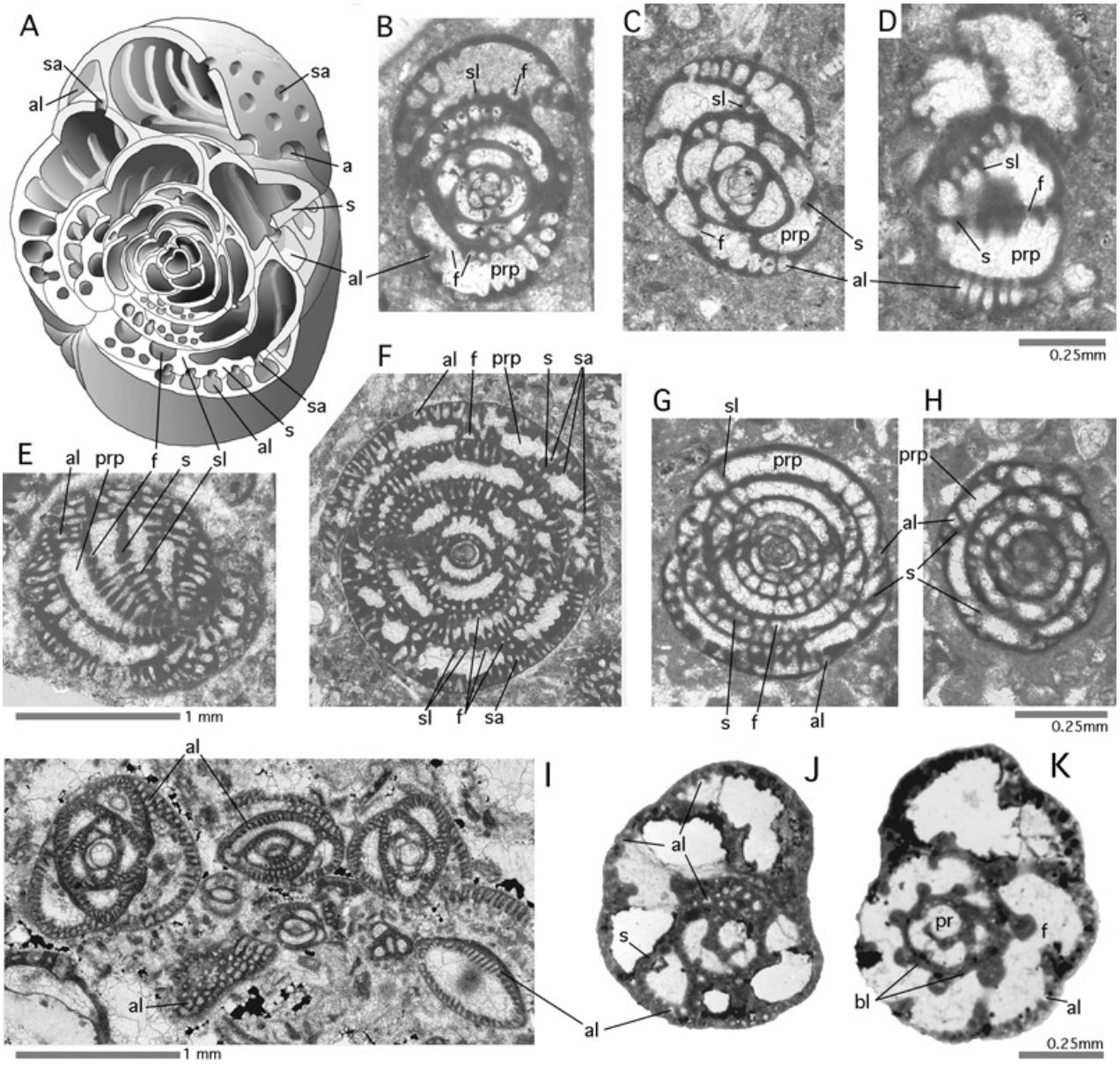

Figure 9: Alveoles.
A-D: model (schematic, not to scale) of the genus *Malatyna* SIREL, subaxial, subequatorial and tangential sections. Igualada, North-Eastern Spain. Uppermost Middle Eocene. **E-F:** *Globoreticulina iranica* RAHAGHI, tangential and axial sections. Shiraz, Iran. Middle-Upper Eocene. **G-H:** *Bullalveolina bulloides* REICHEL, axial and subequatorial sections. Peribetics, South-Eastern Spain. Lower Oligocene. **I:** *Austrotrillina striata* ADAMS, sections perpendicular to apertural axis and tangential sections. Kirkuk, Iraq. Oligocene. **J-K:** *Everticyclammina virguliana* (KOECHLIN), equatorial sections. Mechra Klila, North-Eastern Morocco, Uppermost Jurassic. All sections transmitted light micrographs.
a: (main) aperture; **al:** alveole; **bl:** basal layer; **f:** (main) foramen; **pr:** proloculus; **prp:** preseptal passage (in these cases extending over most of the chamber lumen); **s:** septum; **sa:** supplementary aperture; **sl:** septular ridges (incomplete septula).

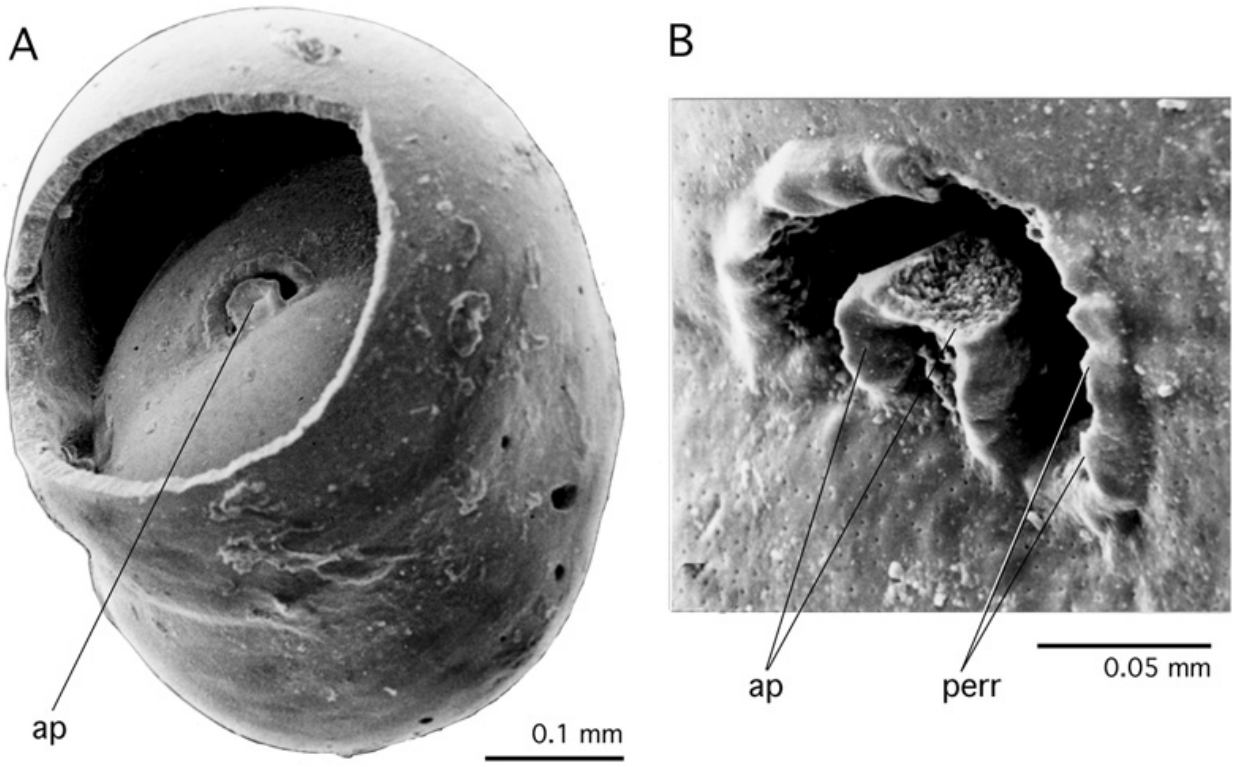

Figure 10: Apertural plate: Apertural feature in *Sphaeroidina bulloides* d'ORBIGNY.
A: dissected specimen showing penultimate foramen, **B:** detail of aperture. SEM graphs. Recent, Gulf of Aqaba. **ap:** apertural plate; **perr:** peristomal, pustulose rim.

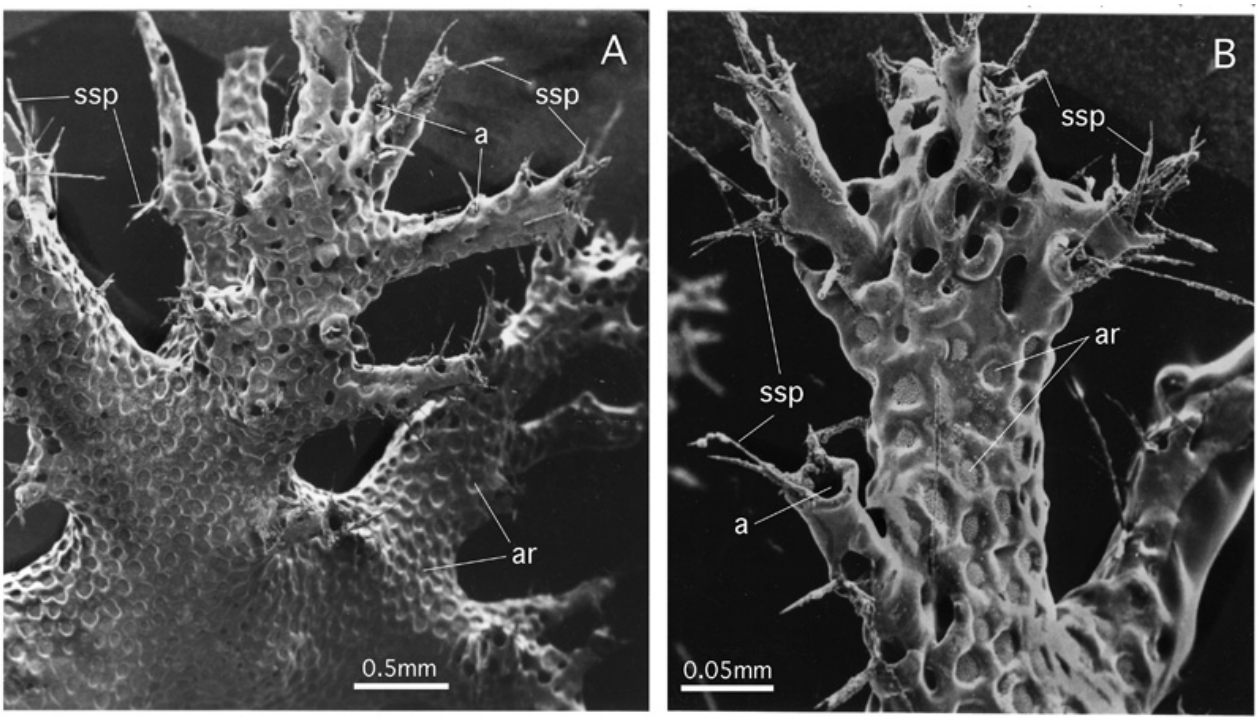

Figure 11: Arborescent shell ornamented by areoli: *Homotrema rubra* (LAMARCK), arborescent habit, SEM graphs, Recent, Gulf of Aqaba.
A: overview of arborescent shell, **B:** detail of a single branch, Note the sponge spicules (**ssp**) glued into the tubular peristomal extension of the aperture to serve as fishing rods that support filiform pseudopodia extending into turbulent water for the capture of food.
a: aperture; **ar:** areoli.

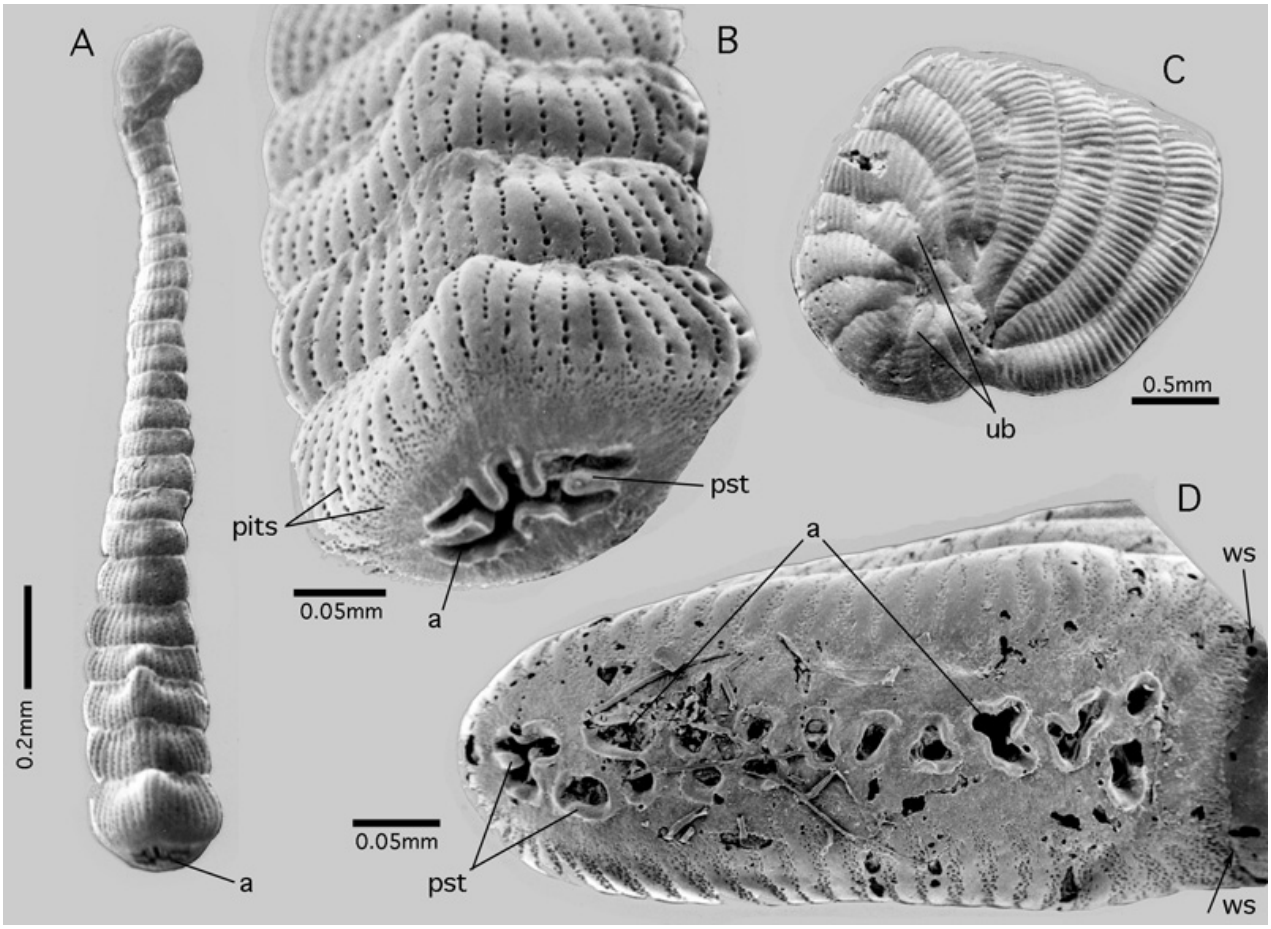

Figure 12: Single and multiple areal apertures.
A-B: *Monalysium acicularis* (BATCH); **C-D:** *Peneroplis planatus* (FICHTEL et MOLL), both from the Gulf of Aqaba, Red Sea, Recent. SEM graphs. Note the presence of pits in the porcelaneous wall and the umbilical bowl characterizing *P. planatus*.
a: areal aperture(s); **pst:** peristomal rims; **ub:** (delimitation of) umbilical bowl; **ws:** whorl suture. Note the absence of interiomarginal apertures.

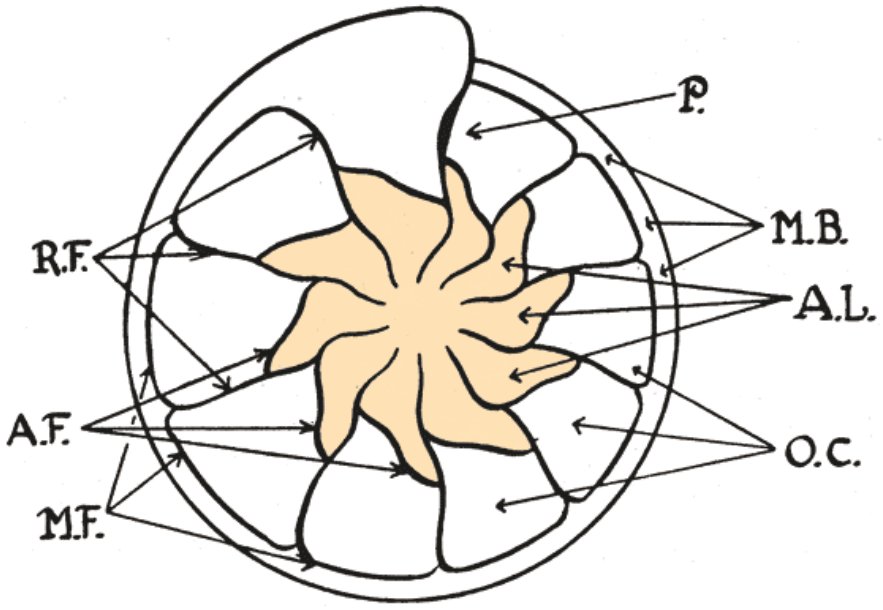

Figure 13: Astral lobes: Original figure from DAVIES, 1932, p. 414.
AF: astral furrow (= foliar suture); **AL** (coloured): astral lobes (= folia): **MB:** marginal band (= keel); **MF:** marginal furrow (= septal suture); **OC:** outer chambers; **P:** pylome (= aperture); **RF:** radial furrows (= chamber sutures).

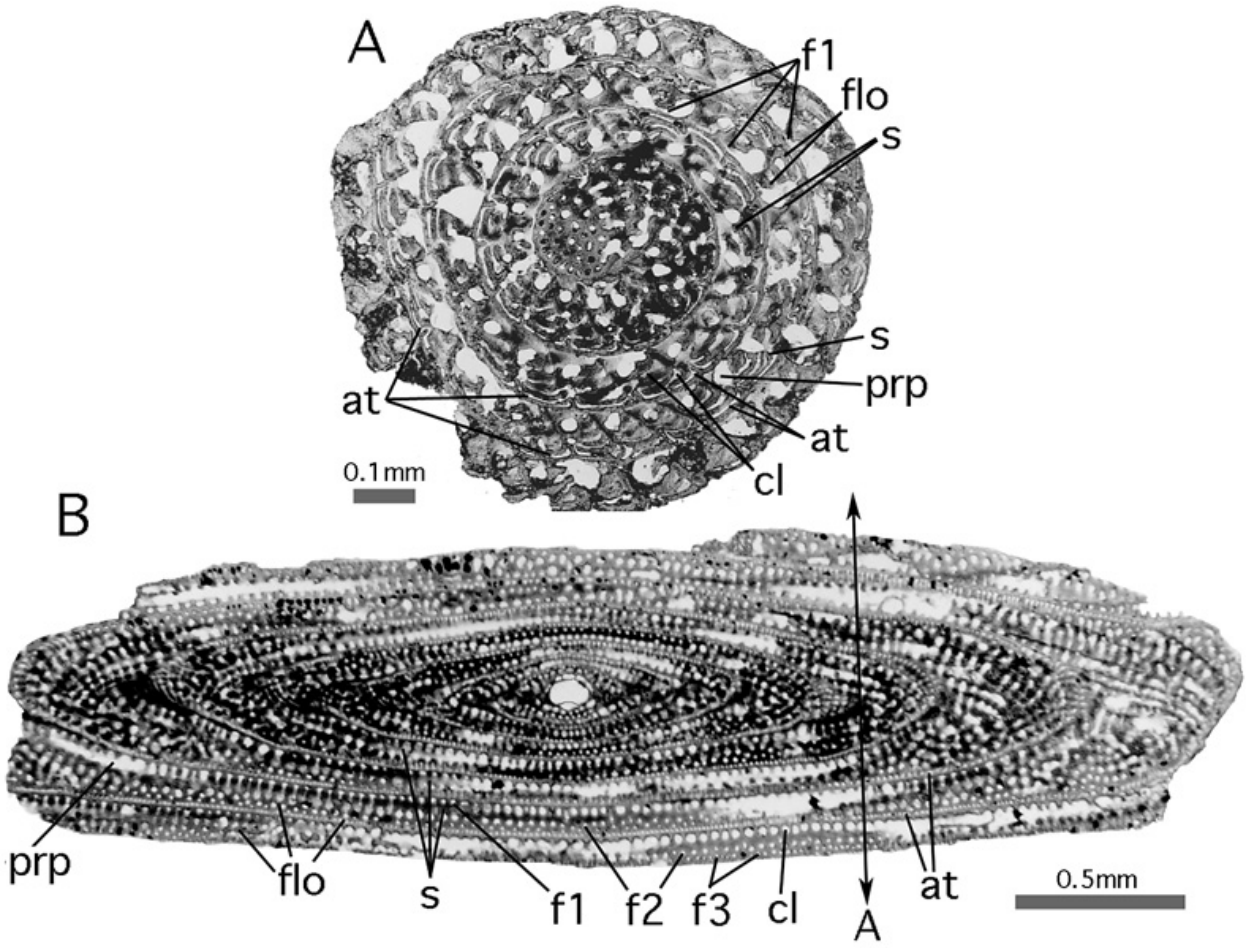

Figure 14: Attics and floors in *Alveolinella borneensis* TAN SIN HOK, Molukkas, Miocene. Transmitted light micrographs.
A: Transverse section. Position in respect to B: double arrow A. **B:** axial section. **at:** attics; **cl:** chamberlet; **f1:** foramen (basal row): **f2:** foramen (second row); **f3:** supplementary foramina corresponding to the attics; **flo:** floors; **s:** septum.

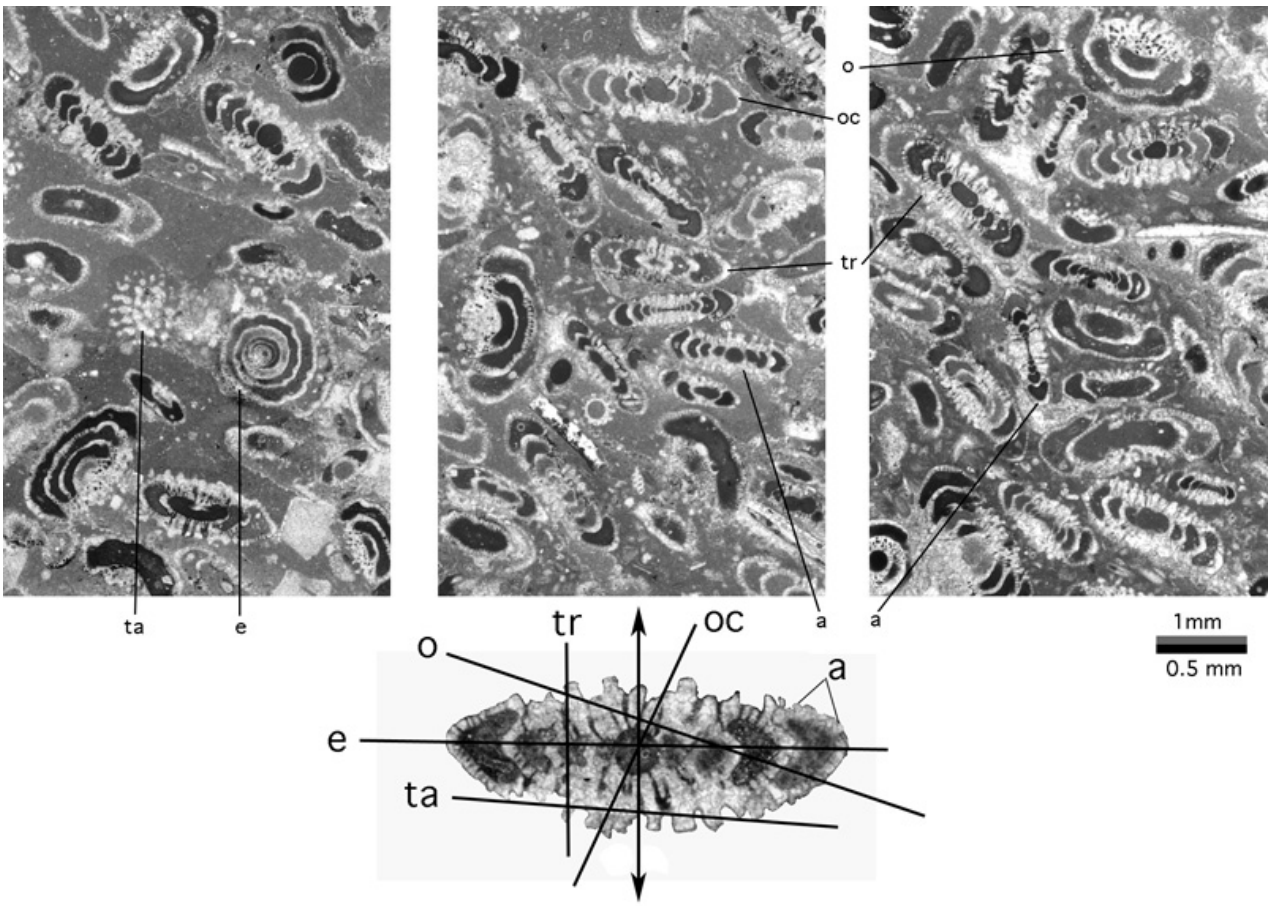

Figure 15: Sections of *Involutina liassica* (JONES). Middle Lias, from Arzo, Ticino, Southern Switzerland. Transparent light micrographs. *Involutina* exhibits a lamellar-perforate, planispiral-evolute, dimorphic shell with a spherical megalosphere followed by a tubular chamber cavity without septa. Lateral walls ornamented by protuberant piles between coarse pores. Double arrow: shell axis.
a: axial section; **e:** equatorial section; **o:** oblique section; **oc:** oblique-centered section; **ta:** tangential section; **tr:** transverse section.

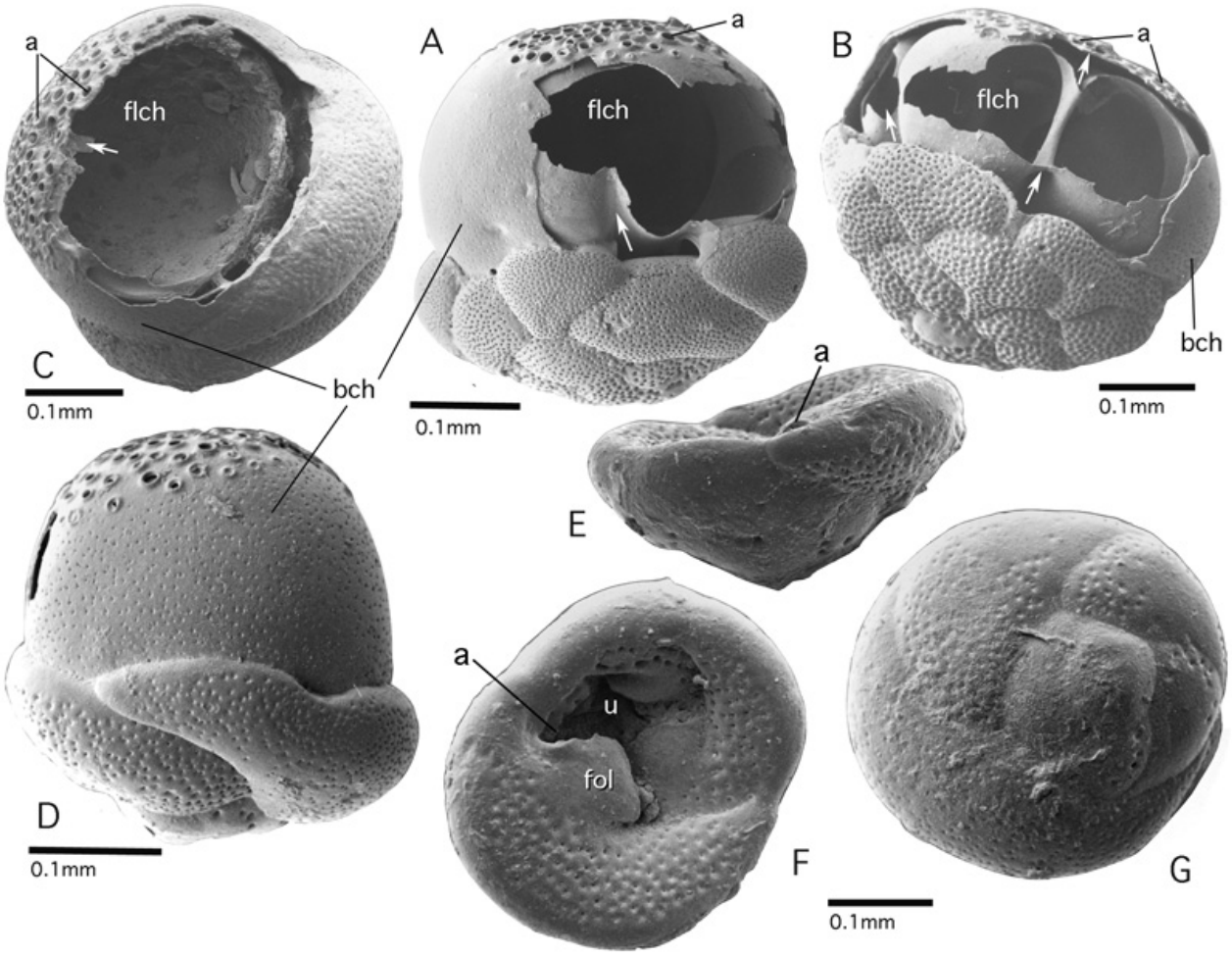

Figure 16: Balloon and float chambers in pseudoplanktic forms. All specimens from the Gulf of Aqaba, Red Sea, Recent. SEM graphs.
A-B: *Cymbaloporetta* sp. Lateral views of dissected specimens. Note tubular infolds of the float chamber canalizing the hatching from the umbilical cavity to the preseptal space under the apertures of the balloon chamber (**arrows**). **C-D:** *Tetromphalus bulloides* (d'ORBIGNY). Lateral views of dissected and intact specimens in their pseudoplanktic stage. **E-G:** *T. bulloides* in its benthic stage, showing open umbilicus, lateral, umbilical (ventral) and spiral (dorsal) views.
a: aperture; **bch:** balloon chamber; **flch:** float chamber; **fol:** folium; **u:** umbilicus.

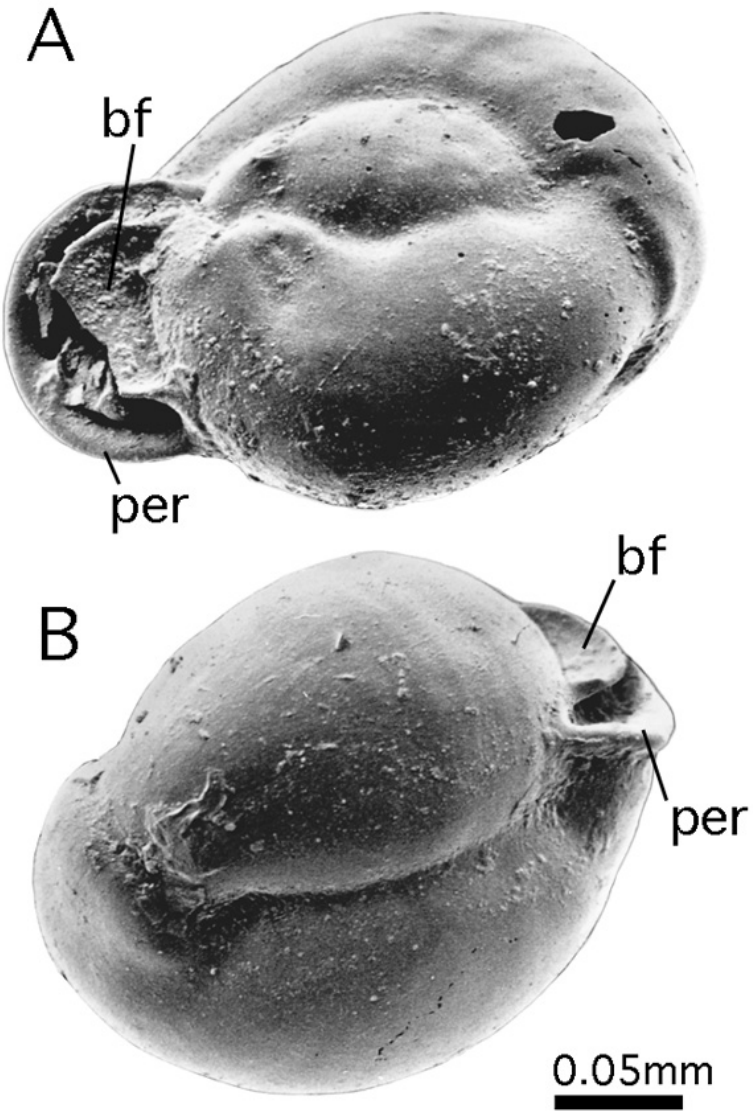

Figure 17: Basal flap in *Miliolinella* sp. from the Gulf of Aqaba. Recent. SEM graphs.
bf: basal flap; **per:** peristomal lip, everted.

Figure 18: Basal layer and flosculinisation. ▶
A: Unidentified, large miliolid, *Fabularia roselli* CAUS and *Dendritina* sp. Randomly oblique sections. Uppermost Middle Eocene, Spanish Pyrenees. **B:** *Idalina antiqua* MUNIER-CHALMAS et SCHLUMBERGER. More or less centered, subaxial sections. Santonian, Spanish Pyrenees. Note the proloculus wall illustrating the reduced thickness of the outermost layer of the primary chamber wall. The difference in the opacities of the basal layer and the primary outer chamber wall demonstrates how dissimilarly the discrete submicroscopic, porcelaneous wall textures react to diagenesis. **C:** *Fabularia verseyi* COLE, oblique section, from Jamaica, Middle Eocene, showing irregular tubiform, anastomosing passages in the basal layer. **D-F:** random sections of *Pseudochubbina globularis* (SMOUT), subspherical, and *P. kassabi* DE CASTRO, flaring, showing parallel, rarely anastomosing tubiform passages in the basal layer, and an outer layer of more regular parallel chamberlets similar to attics, as also in *Fabularia*. Note the thin spirotheca extending into a lateral cover of the flaring portion of the test. Campanian, Iran. **G:** *Alveolina daniensis* DROBNE, oblique sections near the equatorial plane. Compaction of the sediment has mechanically separated outer from inner whorls, revealing the thin spirotheca. Note lines of accretion parallel to the septum in the basal layer of flosculinized whorls. Lowermost Eocene, Slovenia. **H:** *Alveolina tenuis* HOTTINGER, axial section, showing columella produced by polar thickening of the basal layer. Note tubular passages in the columella, continuous in subsequent chambers, without interruption by preseptal spaces. Middle Eocene, Aquitaine, Southwestern France.
Abbreviations: **bl:** basal layer; **prp:** preseptal space or passage; **s:** septum; **spth;** spirotheka (outer wall of sucessive spiral chambers); **tph:** trematophore. Scale bars: 1mm.

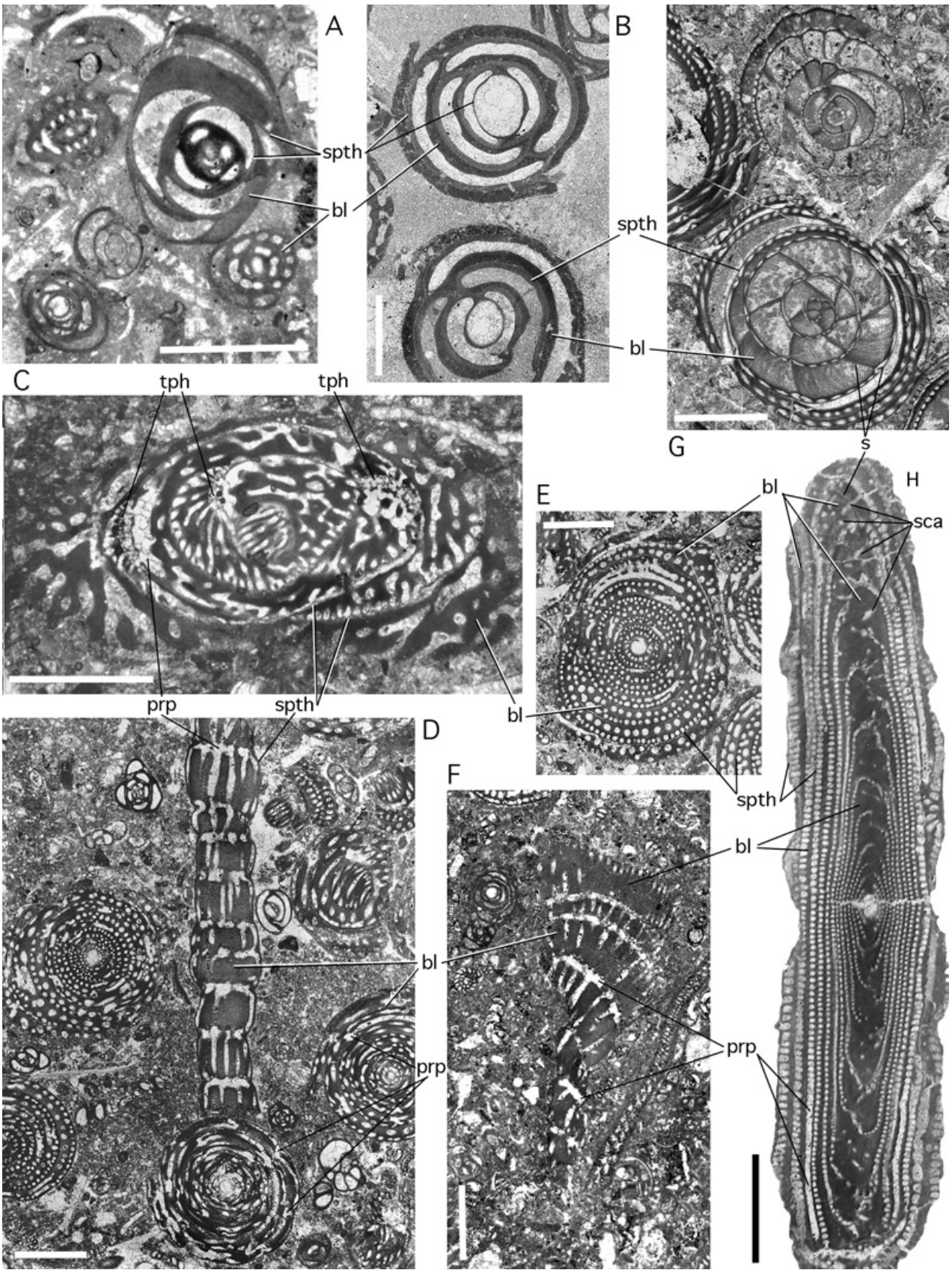
A
spth
bl
B
spth
bl
C
tph
tph
prp
spth
D
bl
prp
E
bl
spth
F
bl
prp
G
s
H
bl
sca

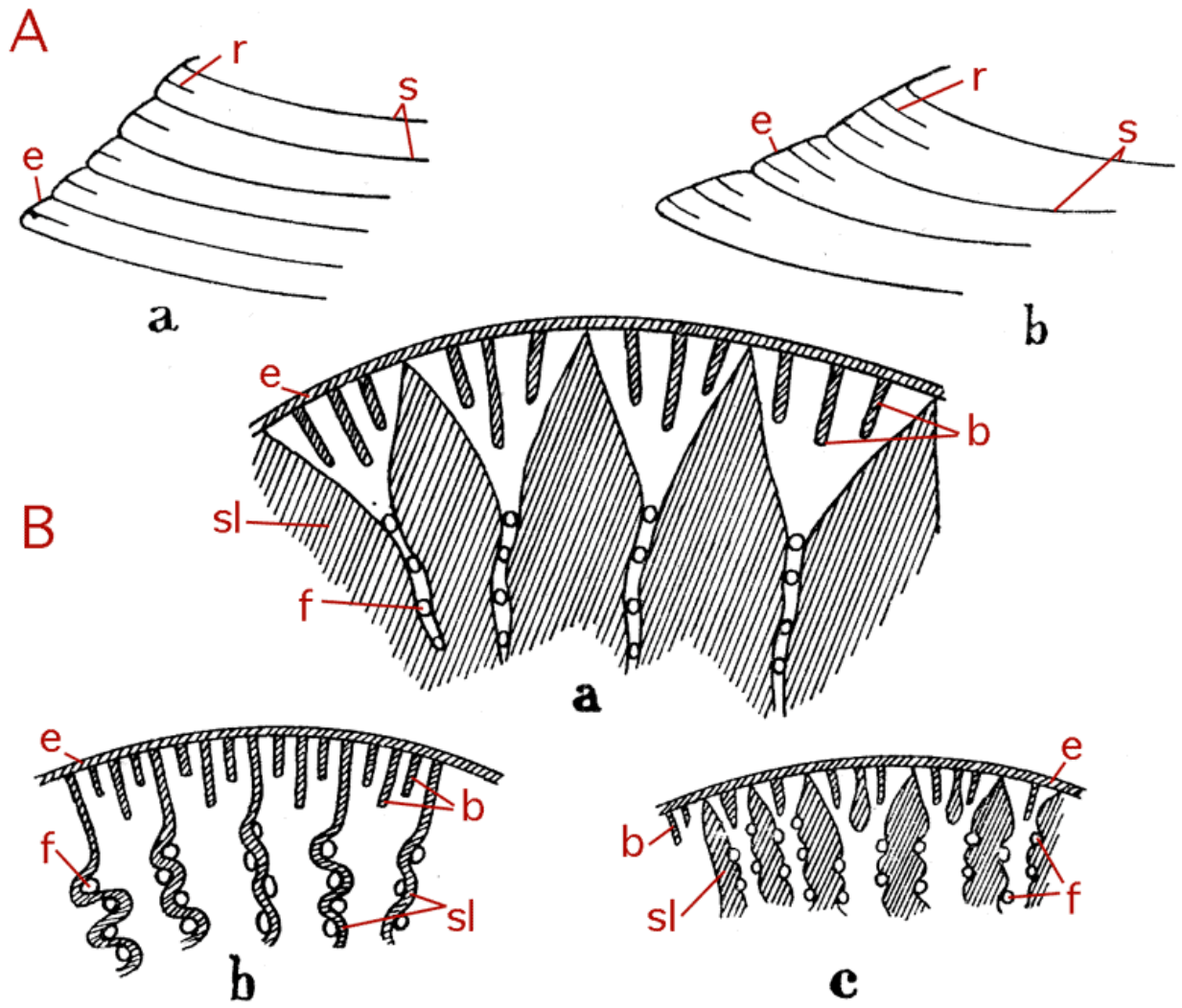

Figure 19: HENSON's "subepidermal partitions" (1948, text-figs. 6-7).
A: axial sections of uniserial cones (as in Orbitolinidae) with (a) "primary subepidermal plates" and (b) with "primary and secondary subepidermal plates". **B:** basal sections of radial zone showing in addition to "radial plates" (a) "thick, straight radial partitions, (b) "thin radial partitions in zigzag" and (c) "subepidermal plates thickening inward". Compare Fig. 71.
Current interpretation given in red: **b:** beam (perpendicular to septum); **e:** epiderm; **f:** foramina (in Orbitolinines forming a crosswise-oblique pattern); **r:** rafter (parallel to septum); **s:** septum; **sl:** septulum (may fuse with beam).

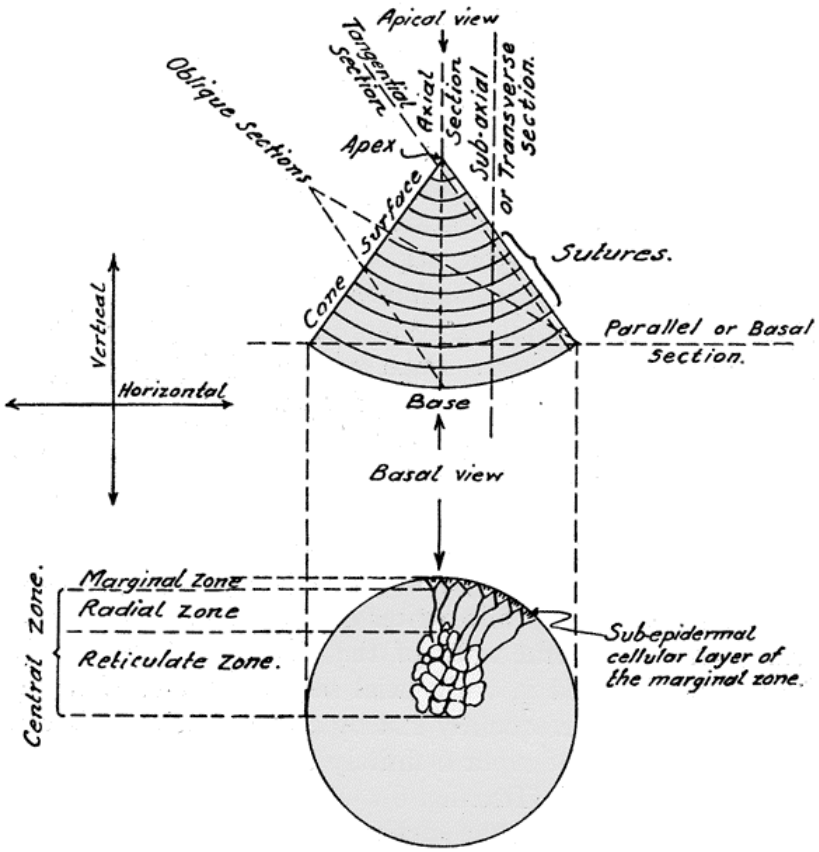

Figure 20: HENSON'S "zonation" of discoidal chambers in uniserial-conical shells, namely the marginal, radial and reticulate zones. Compare Fig. 71. From HENSON, 1948.

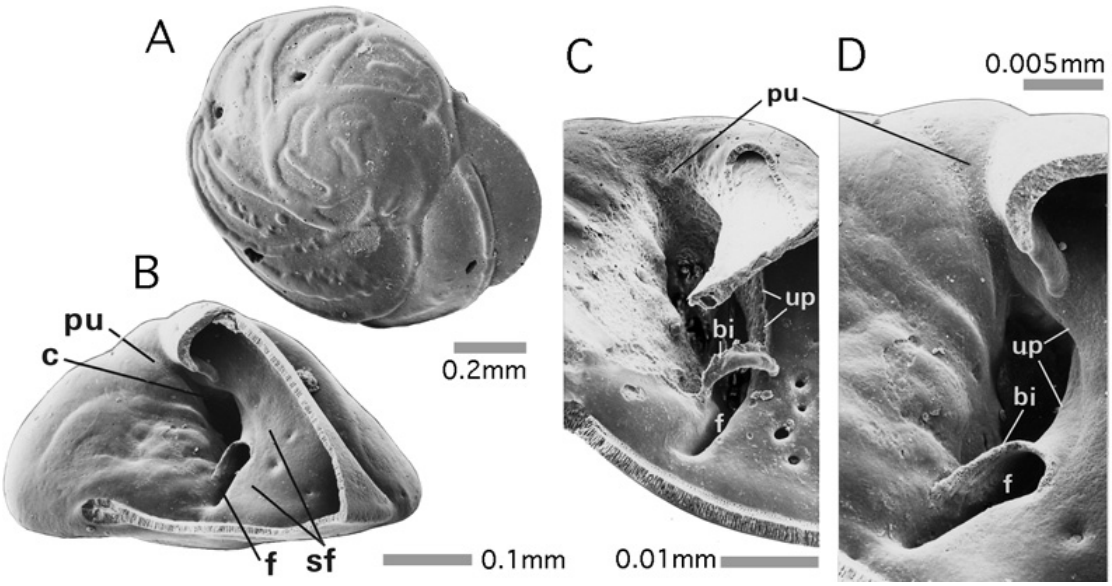

Figure 21: Bipartitor and pseudoumbilicus in *Eponides repandus* (FICHTEL et MOLL) from the Gulf of Aqaba, Red Sea, Recent. SEM graphs.
A: dorsal (spiral) view, **B:** lateral view of dissected specimen. **C:** oblique umbilical view of dissected specimen. **D:** detail of rotated oblique umbilical view.
bi: bipartitor; **c:** spiral umbilical canal; **f:** foramen; **pu:** pseudoumbilicus; **sf:** septal face: note supplementary apertures closed by septal flap covering the septal face; **up:** umbilical plate.

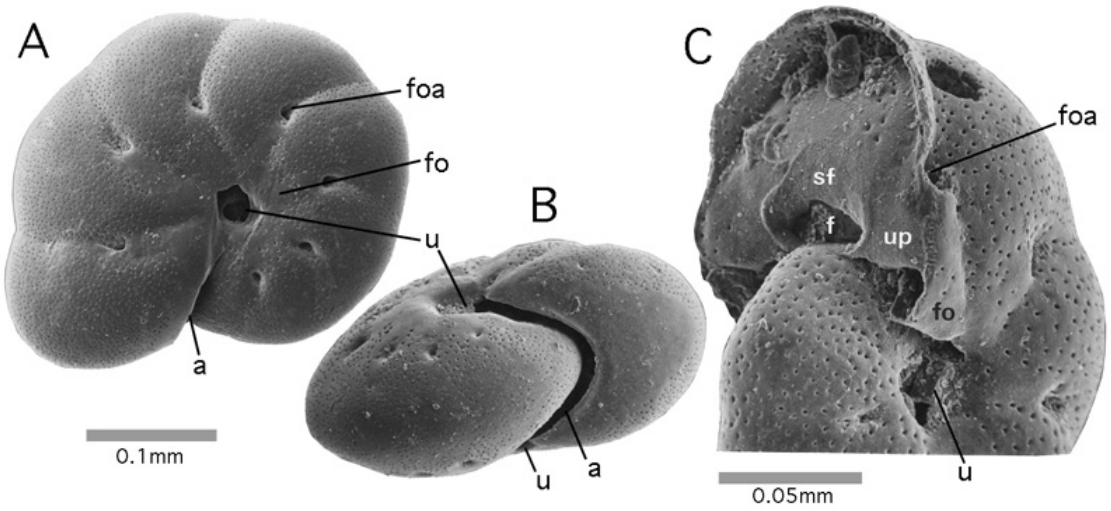

Figure 22: Biumbilicate shell in *Astrononion* sp. from the Gulf of Aqaba, Red Sea, Recent. SEM graphs.
A: lateral view; **B:** apertural view; **C:** oblique view of dissected specimen showing structural details. **a:** aperture; **f:** foramen; **fo:** folium; **foa:** foliar aperture; **sf:** septal face, covered by septal flap; **up:** umbilical plate; **u:** umbilicus, on both sides of the test.

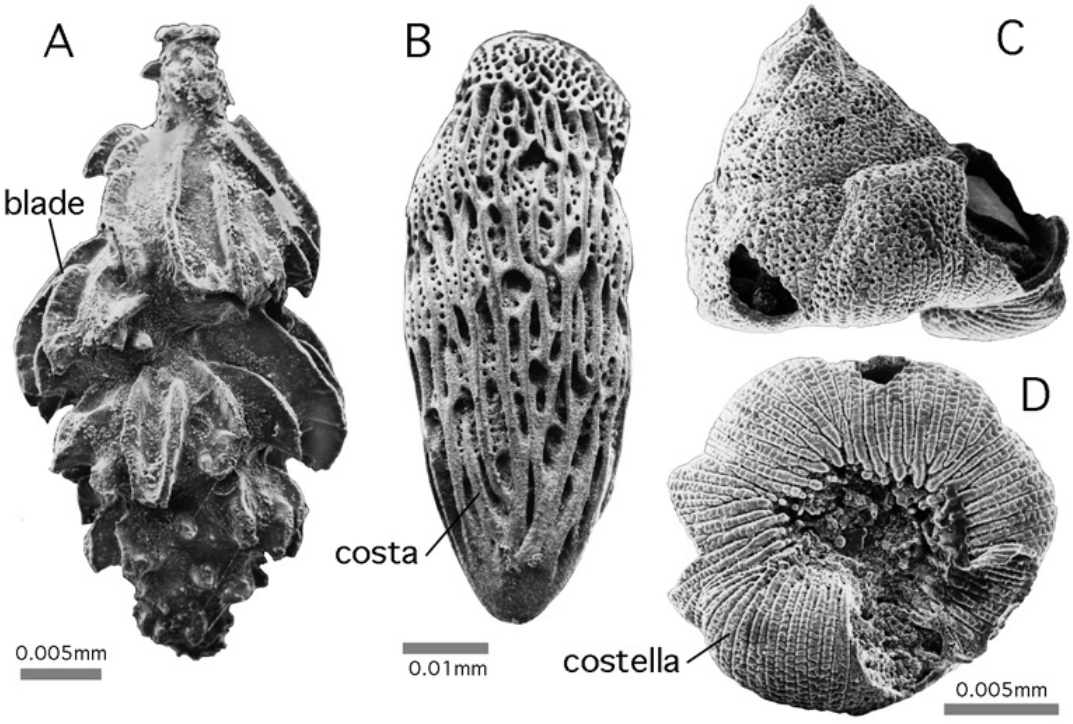

Figure 23: Blades, costae and costellae, linear-elongate ornaments of lamellar-perforate shells.
A: *Neouvigerina porrecta* (BRADY), lateral view; **B:** *Loxostoma amygdalaeformis* (BRADY), lateral view; **C-D:** *Glabratellina* sp., lateral and umbilical views. SEM graphs. Gulf of Aqaba. Recent.

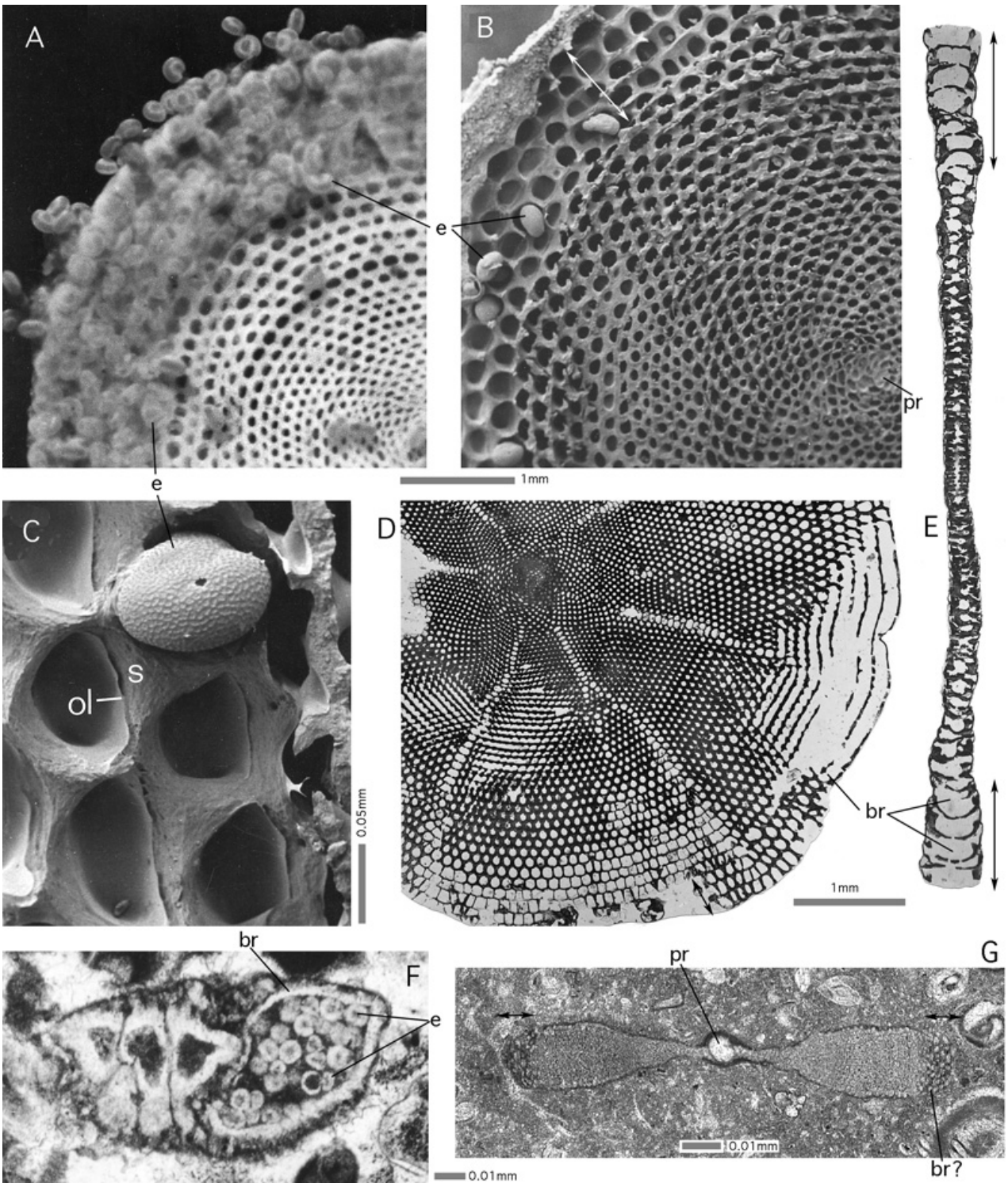

Figure 24: Brood chambers in agamonts of (**A-C**) *Sorites orbiculus* (FORSKAL) and (**D-E**) *Amphisorus hemprichii* EHRENBERG, all from the Gulf of Aqaba. Recent.
A: fresh hatching on empty mother shell under water. **B:** agamont shell, dried and split open in the equatorial plane. Some embryos remain in situ in the brood chambers. Note size of microspheric proloculus. SEM graph. **C:** detail of B showing embryo (consisting of proloculus and flexostyle) and surface of resorption including the organic lining. **D:** equatorial and **E:** axial sections showing an abrupt increase in the irregularity and volume of the chamberlet cavity in the last few chamberlet cycles (**double arrows**) marking the brood chambers. **F:** *Neorotalia* sp., thin section parallel to and near the axis of coiling, the last chamber filled with hatchlings. Transparent light micrograph. Spanish Pyrenees, Lower Eocene. **G:** *Orbitolites* sp. Oblique-centered thin section, transmitted light micrograph. Note the discrepancy between embryo size and brood chamberlet volumes: we are in presence of either a gamont producing small gametes or zygotes, or of a schizont keeping the offspring in regular broodchambers prior to the first, prolocular shell formation. Lowermost Eocene, Farafrah Oasis, Egypt.
br: brood chamber; **e:** embryo; **ol:** organic lining; **pr:** proloculus; **s:** septum.

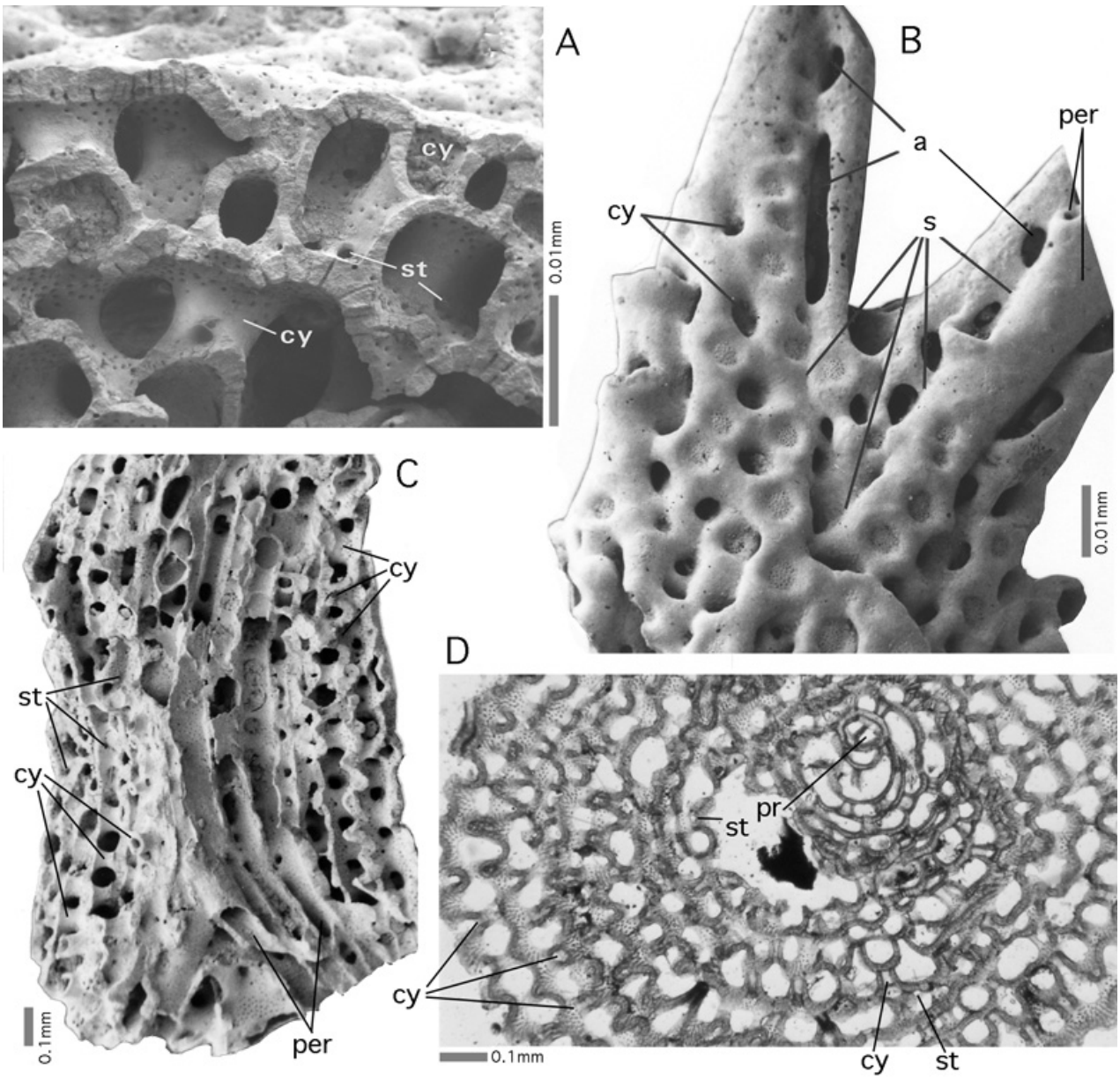

Figure 25: Calyces in arborescent *Miniacina miniacea* (PALLAS) from the Gulf of Aqaba. Recent.
A: Fragment broken perpendicularly with respect to the axis of the branch, showing an exterior view of the broken funnel walls of the calyces. SEM graph. **B:** External view of a branch tip showing calyces and apertures at the limiting suture of the expanse chamber that covers previously formed tubular peristomes. SEM graph. **C:** Fragment broken in the axial plane of branch. SEM graph. **D:** Thin section perpendicular to the stem axis of the shell. Transmitted light micrograph. Calyces cut obliquely produced characteristic undulating intersections.
a: apertures in marginal position, to be transformed into stolons when overgrown by a subseqent expanse chamber; **cy:** calyx; **per:** tubular peristome either terminal or overgrown by subsequent expanse chambers; **pr:** proloculus; **s:** marginal suture of expanse chamber; **st:** stolon.

Figure 26: Canal systems. ▶
A: basic geometry of canals in simple rotaliid shells. Schematic, not to scale. **Red:** chamber plasm; **yellow:** canal plasm. **B-C:** during stages of retraction of the chamber plasm into the interior of the shell, the canal system provides motility to the organism by extruding the pseudopods through backdoors, so-called loop-holes. **D-F:** *Challengerella bradyi* BILLMAN *et alii*. Gulf of Aqaba, Red Sea; Recent. SEM graphs. **D:** oblique-ventral view of umbilical face; **E:** dorsal (spiral) view; **F:** Epoxy resin cast of shell cavities showing canal system. **G–H:** *Hottingerella chouberti* (HOTTINGER), Northeastern Morocco, Lower Cretaceous. Schema after HOTTINGER, 1976, not to scale, and transmitted light micrographs. Note that the basic geometry with loop-holes in a shell lacking septal subdivision is similar to a rotaliid with chambers.
a: aperture: **ch:** chamber; **f:** foramen; **fol:** folium; **is:** interlocular, intraseptal space; **isc:** ingtraseptal canal; **lh:** loop-hole; **m:** mask; **p:** pores; **rmfu:** radial marginal furrows (open to the ambient environment for their full length prior to being covered by the next whorl); **s:** septum; **sesut:** septal sutures; **sis:** spiral interlocular space; **spc:** spiral canal; **spmfu:** spiral marginal furrow; **spsut:** spiral suture (between successive whorls); **up:** umbilical plate (general geometric position); **vc:** vertical canals (at umbilical chamber suture); **x:** approximate position of section.

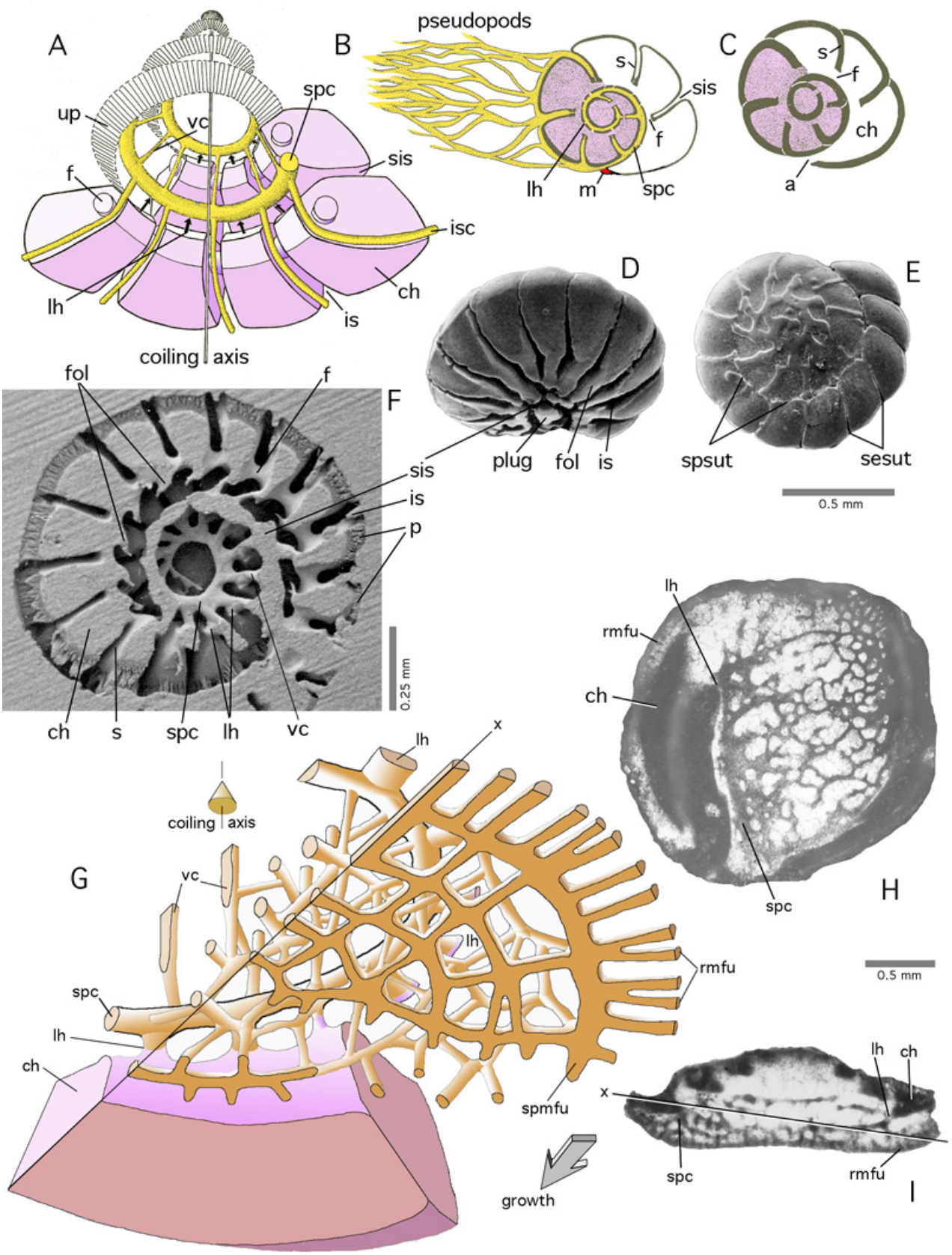
A
up
vc
spc
sis
f
isc
ch
lh
is
coiling axis
B
pseudopods
s
sis
f
lh
m
spc
C
s
f
ch
a
D
plug
fol
is
E
spsut
sesut
0.5 mm
F
fol
f
sis
is
p
ch
s
spc
lh
vc
0.25 mm
G
coiling axis
lh
x
vc
lh
rmfu
spc
lh
ch
spmfu
growth
H
lh
rmfu
ch
spc
0.5 mm
I
lh
ch
x
spc
rmfu

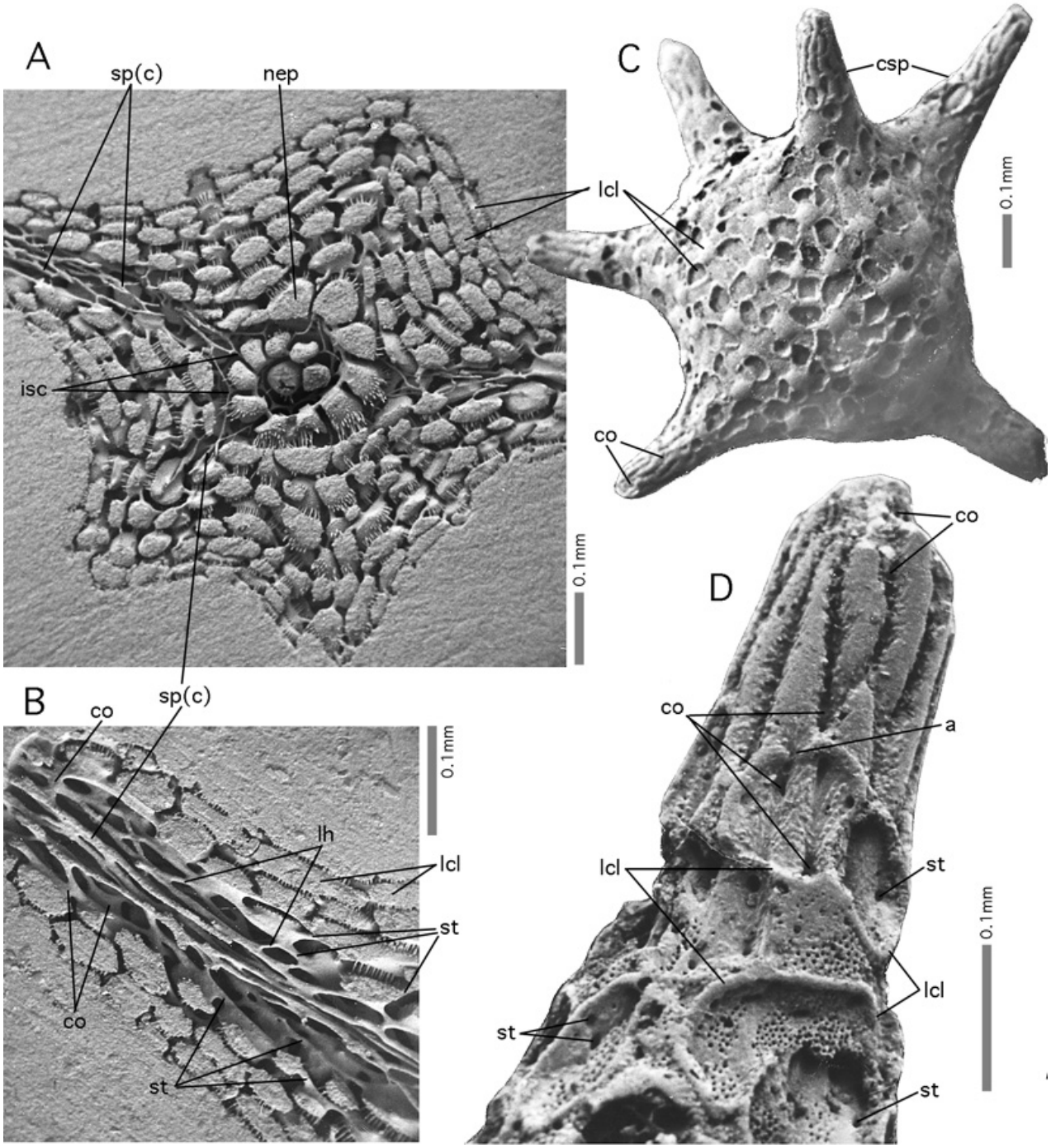

Figure 27: Canaliferous spines in *Baculogypsina sphaerulata* (PARKER et JONES), Keij Island, Indonesia. Recent. SEM graphs.
A-B: Epoxy resin casts of shell cavities, the mineralized shell having been dissolved, showing that spine canals originate as extensions of an intraseptal interlocular space, that is then transformed into canals. They feed in their turn the supplemental chamberlets overgrowing the base of the spine. **C-D:** Shell showing chessboard pattern of supplemental chamberlets, overgrowing the base of the canalled spine and fed in part by the overgrown canal orifices.
a: aperture (of lateral chamberlet); **co:** canal orifice; **csp:** canalicular spine; **lcl:** lateral chamberlet; **lh:** loop-hole; **nep:** (spiral) nepiont; **sp(c):** spine canals; **st:** stolon.